Synthesis and Structure of Titanocene Complexes with η^2-Coordinated Internal Ferrocenylacetylenes

Petr Štěpnička, Róbert Gyepes, and Ivana Císařová

Department of Inorganic Chemistry, Charles University, Hlavova 2030, 128 40 Prague 2, Czech Republic

Vojtech Varga,‡ Miroslav Polášek, Michal Horáček, and Karel Mach*

J. Heyrovský Institute of Physical Chemistry, Academy of Sciences of the Czech Republic, Dolejškova 3, 182 23 Prague 8, Czech Republic

Received October 5, 1998

The reduction of $(\eta^5\text{-}C_5H_{5-n}Me_n)_2TiCl_2$ (n = 0, 4, and 5) complexes by magnesium metal in tetrahydrofuran and in the presence of [(trimethylsilyl)ethynyl]ferrocene (**2**) or [(phenyl)-ethynyl]ferrocene (**3**) affords the $(\eta^5\text{-}C_5H_{5-n}Me_n)_2Ti(\eta^2\text{-}FcC{\equiv}CR)$ complexes [Fc = $(\eta^5\text{-}C_5H_5)$-Fe$(\eta^5\text{-}C_5H_4)$, R = $SiMe_3$ (**4**−**6**) and Ph (**7**−**9**)]. Crystal structures of **5** and **9** show a titanacyclopropene-like mode of coordination of the acetylenes **2** and **3.** Bonding of the acetylenes to the titanocene unit results in a remarkable downfield shift of ^{13}C NMR resonances of the acetylenic carbon atoms and in a large red shift of the ν(C≡C) wavenumbers. Testing the complexes **6** and **9** toward head-to-tail dimerization of HC≡CSiMe_3 showed that compound **9** induces dimerization to give exclusively 2,4-bis(trimethylsilyl)-but-1-en-3-yne (**10**), whereas complex **6** is inactive.

Introduction

Compounds in which two or more transition metals are linked by an organic chain are capable of intramolecular electron transfer and may also serve as starting compounds for synthesis of metal-rich polymers and other conductive and/or nonlinear optical materials.[1] In contrast to numerous late−late transition metal complexes reported so far,[2] the compounds involving early−late transition metal combinations are relatively rare.[3] Moreover, if binuclear early−late complexes are to be applied as catalysts in C−C bond formation reactions of olefins and acetylenes, the linking groups should not contain hard donors (such as O, N) since highly electrophilic early transition metals (Ti, Zr, Hf) are deactivated by forming strong metal−hard donor bonds. As far as the titanocene and ferrocene moieties are concerned, known combinations are represented by titanocene bis(ferrocenylacetylide) $[(\eta^5\text{-}C_5H_4(SiMe_3)]_2Ti(\eta^1\text{-}C{\equiv}CFc)_2$ and its tweezer complex with an embedded Ni(CO) group,[4] and by titanocene bis(acetylide) complexes $(\eta^5\text{-}C_5H_4R)_2Ti[\eta^1\text{-}(C{\equiv}C)_nFc]_2$ (n = 1, 2).[5] Recently, a directly ring-to-ring linked pseudotitanocene−ferrocene complex, (η^5-1,2,5,6-tetrakis(trimethylsilyl)(4-ferrocenyl)cyclohexa-1,4-dienyl)(η^5-cyclopentadienyl)titanium(II) $[(\eta^5\text{-}(Me_3Si)_4FcC_6H_2\}Ti(\eta^5\text{-}C_5H_5)]$, was obtained in a cyclohexadienyl ligand-forming reaction.[6]

Herein we describe alternative syntheses of ferrocenylacetylenes **2** and **3** and the synthesis and full spectral characterization (NMR, IR, UV/vis, MS) of their titanocene complexes $(\eta^5\text{-}C_5H_{5-n}Me_n)_2Ti(\eta^2\text{-}FcC{\equiv}CR)$ [n = 0, 4, and 5; Fc = ferrocenyl $(\eta^5\text{-}C_5H_5)Fe(\eta^5\text{-}C_5H_4)$; R = $SiMe_3$ (**4**−**6**) and Ph (**7**−**9**)]. Solid-state structures of **5** and **9** and the catalytic activity of **6** and **9** toward selective head-to-tail dimerization of (trimethylsilyl)-acetylene (TMSA) are also reported.

Results and Discussion

Lithiation of ethynylferrocene, **1**, with *n*-BuLi followed by metathesis of the resulting lithioacetylene with chlorotrimethylsilane gave [(trimethylsilyl)ethynyl]ferrocene, **2**, in nearly quantitative yield. [(Phenyl)ethynyl]-ferrocene, **3**, was obtained in 89% yield by Pd/Cu-catalyzed cross-coupling[7] of acetylene **1** with iodobenzene

* To whom correspondence should be addressed. E-mail: mach@jh-inst.cas.cz.

‡ Present address: Synthetic Rubber Research Institute, Kaučuk a. s., 278 42 Kralupy nad Vltavou, Czech Republic.

(1) (a) Long, N. J. *Angew. Chem., Int. Ed. Engl.* **1995**, *34*, 21. (b) Colbert, M. C. B.; Lewis, J.; Long, N. J.; Raithby, P. R.; Younus, M.; White, A. J. P.; Williams, D. J.; Payne, N. N.; Yellowless, L.; Beljonne, D.; Chawdhurry, N.; Friend, R. H. *Organometallics* **1998**, *17*, 3034.

(2) (a) Fe/Rh: Wiedemann, R.; Fleischer, R.; Stalke, D.; Werner, H. *Organometallics* **1997**, *16*, 866. (b) Ru/Pd, Fe/Pd: Lavastre, O.; Plass, J.; Bachmann, P.; Guesmi, S.; Moinet, C.; Dixneuf, P. H. *Organometallics* **1997**, *16*, 184. (c) Fe/Ru: Štěpnička, P.; Gyepes, R.; Lavastre, O.; Dixneuf, P. H. *Organometallics* **1997**, *16*, 5089. (d) Fe/Ru: Long, N. J.; Martin, A. J.; de Biani, F. F.; Zanello, P. *J. Chem. Soc., Dalton Trans.* **1998**, 2017. (e) Fe/Ru: Jones, N. D.; Wolf, M. O.; Giaquinta, D. M. *Organometallics* **1997**, *16*, 1352. (f) Fe/Pt: Sato, M.; Mogi, E.; Kumakura, S. *Organometallics* **1995**, *14*, 3157. (g) Fe/Fe: Sato, M.; Hayashi, Y.; Kumakura, S.; Shimizu, N.; Katada, M.; Kawata, S. *Organometallics* **1996**, *15*, 721.

(3) (a) Zr/Ru: Lemke, F. R.; Szalda, D. J.; Bullock, R. M. *J. Am. Chem. Soc.* **1991**, *113*, 8466. (b) Hf/Fe: Back, S.; Rheinwald, G.; Zsolnai, L.; Huttner, G.; Lang, H. *J. Organomet. Chem.* **1998**, *563*, 73.

(4) Back, S.; Pritzkow, H.; Lang, H. *Organometallics* **1998**, *17*, 41.

(5) (a) Hayashi, Y.; Osawa, M.; Kobayashi, K.; Wakatsuki, Y. *J. Chem. Soc., Chem. Commun.* **1996**, 1617. (b) Hayashi, Y.; Osawa, M.; Wakatsuki, Y. *J. Organomet. Chem.* **1997**, *542*, 241.

(6) Štěpnička, P.; Podlaha, J.; Horáček, M.; Polášek, M.; Mach, K. *J. Organomet. Chem.*, in press.

(7) (a) Lavastre, O.; Cabioch, S.; Dixneuf, P. H.; Vohlídal, J. *Tetrahedron* **1997**, *53*, 7595. (b) Lavastre, O.; Ollivier, L.; Dixneuf, P. H.; Sibandhit, S. *Tetrahedron* **1996**, *52*, 5495.

10.1021/om980832u CCC: $18.00
Publication on Web 01/20/1999

Scheme 1. Synthesis of Ethynylferrocenes 2 and 3

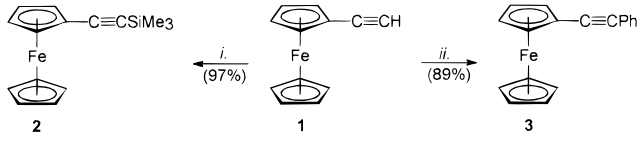

Key: *i.* (a) *n*-BuLi/Et_2O, (b) Me_3SiCl; *ii.* PhI/CuI/[$Pd(PPh_3)_2Cl_2$]/Et_2NH

Scheme 2. Synthesis of η^2-Alkyne Complexes 4−9

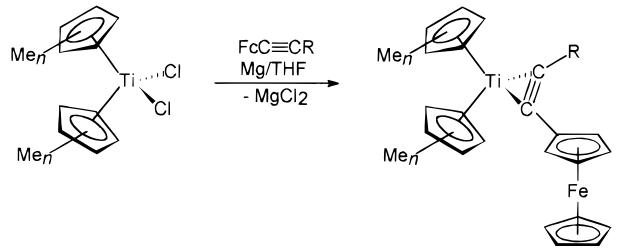

R	*n* = 0	4	5
$SiMe_3$	**4**	**5**	**6**
Ph	**7**	**8**	**9**

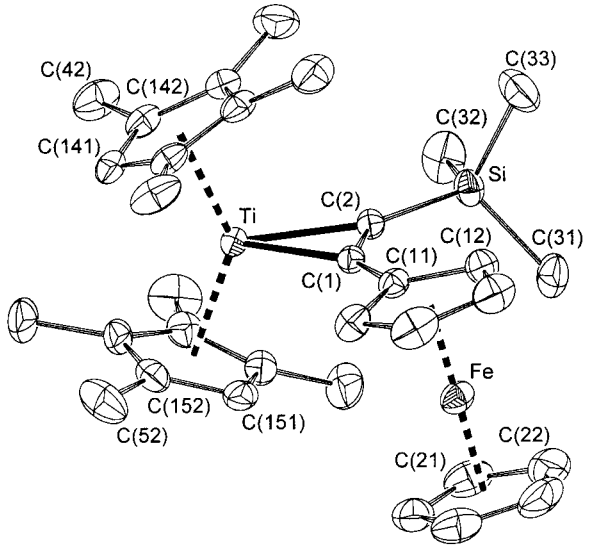

Figure 1. Molecular structure of **5**; thermal ellipsoids correspond to the 30% probability level. All hydrogen atoms were omitted and only pivot and adjacent carbon atoms were labeled for clarity.

(Scheme 1). The alkynes **2** and **3** were reacted with methylated titanocene dichlorides $(\eta^5\text{-}C_5H_{5-n}Me_n)_2TiCl_2$ (n = 0, 4, and 5) in the presence of magnesium turnings in tetrahydrofuran to give the corresponding η^2-alkyne complexes $(\eta^5\text{-}C_5H_{5-n}Me_n)_2Ti(\eta^2\text{-FcC}{\equiv}CR)$ **4**−**6**, **8**, and **9** in good yields after purification (Scheme 2). NMR and MS spectra of the crude products showed the presence of minor impurities due to reduction of the starting alkynes (*E*)-FcCH=CHR and $FcCH_2CH_2R$ (R = $SiMe_3$, Ph). Unfortunately, the crude product resulting from the reaction of $(\eta^5\text{-}C_5H_5)_2TiCl_2$ and **3** was found reproducibly to contain these reduced byproducts as major components. Although the complex **7** was identified in the mixture by NMR and MS spectra, all attempts to isolate pure **7** failed. Such a low stability of complex **7** reflects most likely the absence of methyl groups on the titanocene cyclopentadienyls, which protect the η^2-alkyne complex from subsequent reduction and/or decomposition.

^1H and ^{13}C NMR spectra of **4**−**9** are in full accord with the proposed structures and also compatible with the solid-state structure of **5** and **9** determined by single-crystal X-ray diffraction. The ^{13}C NMR signals of both triple-bond carbons of the ferrocenylacetylenes exhibit a large downfield shift upon coordination to the titanocene unit (δ_C 195−218), thus indicating formation of η^2-alkyne complex.[8] A remarkable but significantly smaller coordination shift was also observed for the *ipso* carbon of the substituted ferrocenyl cyclopentadienyl (Cp) ring (compare δ_C ca. 85 to δ_C 65 for the noncoordinated acetylenes). In contrast to analogous complexes $(C_5H_{5-n}Me_n)_2Ti(\eta^2\text{-}Me_3SiC{\equiv}CSiMe_3)$ (n = 0−5), where the δ_C(C≡C) chemical shift increases with the number of methyl substituents on the rings (δ_C 245−249),[9] complexes **4**−**6** show only marginal variation of δ_C(C≡C). On the other hand, ν(C≡C) vibrations in **4**−**9** show a wavenumber decrease on increasing the number of methyl substituents, thus following the same dependence as the mentioned $(C_5H_{5-n}Me_n)_2Ti(\eta^2\text{-}Me_3SiC{\equiv}CSiMe_3)$ complexes. Furthermore, complexes **4**−**6** display a trend of dependence of λ_{max} of the longest wavelength electronic absorption band on the number of methyl groups similar to the above-mentioned complexes (1060 nm for n = 0 and 920 for n = 4, 5),[9] although at shorter wavelengths (880 and 810 nm for n = 0 and 5, respectively). This band, tentatively assigned to a CT d(Ti) → π^*(alkyne) transition,[9] is even more blue-shifted in the spectra of **8** and **9** (710 and 725 nm, respectively).

Crystal Structure Determination. The molecule of **5** exhibits gross features typical for other titanocene complexes with "organic" η^2-alkynes such as $Me_3SiC{\equiv}CSiMe_3$[9] and $PhC{\equiv}CSiMe_3$.[10] At variance, coordinated [(trimethylsilyl)ethynyl]ferrocene is slightly shifted from the plane bisecting the titanocene moiety (Figure 1, Table 1), as manifested by the dihedral angles of the TiC_2 and $(CH_3)_4C_5H$ least-squares planes of 24.1(1)° and 20.8(1)°. Unlike $(C_5HMe_4)_2Ti(\eta^2\text{-}Me_3SiC{\equiv}CSiMe_3)$,[9] the hydrogen-bearing carbon atoms of the C_5HMe_4 ligands in **5** are not directed to the top of the tilt angle, but one of them (C(151)) is directed toward the ferrocenyl moiety. Accordingly, the tilt angle of the cyclopentadienyl rings in **5** is 5.5° lower than that in $(C_5HMe_4)_2Ti(\eta^2\text{-}Me_3SiC{\equiv}CSiMe_3)$. Also, the methyl groups of the titanocene moiety are disposed from the least-squares plane of the cyclopentadienyl ring by a maximum of 0.26 Å.

As a result of steric interactions of acetylene substituents with titanocene cyclopentadienyls, the acetylene ligand is bonded unsymmetrically; the CE(1), Ti, CE(2) plane (CE = centroid of cyclopentadienyl ring) intersects the C(1)−C(2) bond only 0.34 Å from the C(2) carbon atom. The coordinated carbon−carbon triple bond is markedly lengthened up to the value typical for C−C

(8) Burlakov, V. V.; Polyakov, A. V.; Yanovsky, A. I.; Struchkov, Yu. T.; Shur, V. B.; Vol'pin, M. E.; Rosenthal, U.; Görls, H. *J. Organomet. Chem.* **1994**, *476*, 197.

(9) Varga, V.; Mach, K.; Polášek, M.; Sedmera, P.; Hiller, J.; Thewalt, U.; Troyanov, S. I. *J. Organomet. Chem.* **1996**, *506*, 241.

(10) Rosenthal, U.; Görls, H.; Burlakov, V. V.; Shur, V. B.; Vol'pin, M. E. *J. Organomet. Chem.* **1992**, *426*, C53−C57.

Table 1. Selected Bond Lengths [Å], Bond Angles [deg], and Dihedral Angles[a] [deg] for 5

Ti−C(1)	2.073(2)	C(1)−Ti−C(2)	36.24(9)
Ti−C(2)	2.115(2)	Ti−C(2)−Si	152.1(1)
C(1)−C(2)	1.303(3)	Ti−C(1)−C(11)	146.6(2)
C(1)−C(11)	1.459(3)	C(1)−C(2)−Si	137.8(2)
Si−C(2)	1.841(2)	C(2)−C(1)−C(11)	139.3(2)
Si−C(31)	1.868(4)	C(31)−Si−C(32)	108.4(2)
Si−C(32)	1.870(4)	C(31)−Si−C(33)	107.5(2)
Si−C(33)	1.870(4)	C(32)−Si−C(33)	107.4(3)
C(11)−C(1)−C(2)−Si	−6.8(5)		

	$\{(CH_3)_4C_5H\}_2Ti$	Cp_2Fe
CE−CE	3.905(4)	3.305(5)
M−CE	2.098(2), 2.097(2)	1.652(2), 1.654(2)
M−C(Cp)	2.347(3)−2.504(2)	2.019(4)−2.077(2)
M−C(Cp) av	2.41(5)	2.04(2)
C−C(Cp) av	1.405(5)	1.40(2)
(CpTi)−C(CH_3) av	1.504(5)	
∠(Cp,Cp)	44.49(8)	2.21(3)
CE−M−CE	137.2(1)	178.1(2)

[a] CE denotes the centroid of the corresponding cyclopentadienyl ring.

double bonds (compare C(1)−C(2) 1.303(3) Å vs 1.316 Å for C−CH=CH−C;[11] cf. average value for three crystallographically independent molecules of FcC≡CH in the solid state:[12] 1.17 Å). This elongation, typical for titanacyclopropene-like complexes, is accompanied by bending of the originally linear arrangement of the C(Cp)−C≡C−Si moiety, but without any notable torsion [C(Cp)−C≡C 139.3(2), C≡C−Si 137.8(2)°, C(Cp)−C≡C−Si −6.8(5)°]. While the Si atom lies exactly in the TiC_2 plane, the ferrocenyl group is bent outward. The distance of C(11) from the TiC_2 plane is 0.118(5) Å, and the dihedral angle of the TiC_2 plane and its adjacent cyclopentadienyl ring of the ferrocenyl group is 11.6(1)°. The Cp rings of the ferrocenyl group are almost *eclipsed*, with a dihedral angle of their least-squares planes of only 2.21(3)°.

The overall geometry of complex **9** is similar to that of **5** (Figure 2, Table 2). The titanocene cyclopentadienyls are in a staggerred conformation and subtend the dihedral angle of 40.1(2)°. The angle differs from that of $(C_5Me_5)_2Ti(\eta^2\text{-}Me_3SiC{\equiv}CSiMe_3)$[8] by only 1.0°. Methyl groups on the titanocene cyclopentadienyls are bent outward from the titanium center, the perpendicular distance of methyl groups from the cyclopentadienyl plane varying in the range 0.08−0.35 Å. The ferrocene unit adopts a nearly *eclipsed* conformation with the ring tilt angle 5.8(2)°.

In contrast to **5**, the CE(1), Ti, CE(2) plane approximately bisects the coordinated triple bond, and the torsional deformation at the coordinated triple bond is more profound. This is documented by the torsion angle C(11)−C(1)−C(2)−C(31) of 15.8(7)°, by the dihedral angle of the TiC_2 and phenyl planes of 18.3(3)°, and also by a much larger deviation of the ferrocenyl Cp ring and the TiC_2 plane from the parallel arrangement [dihedral angle 34.2(2)°; cf. perpendicular distances to the TiC_2 plane C(31) 0.001(8), C(11) 0.259(7) Å]. The phenyl group is slightly rotated from the TiC_2 plane as follows from the torsion angles C(1)−C(2)−C(31)−C(3*n*); 18.2(7)° for $n = 2$ and −162.2(5)° for $n = 6$.

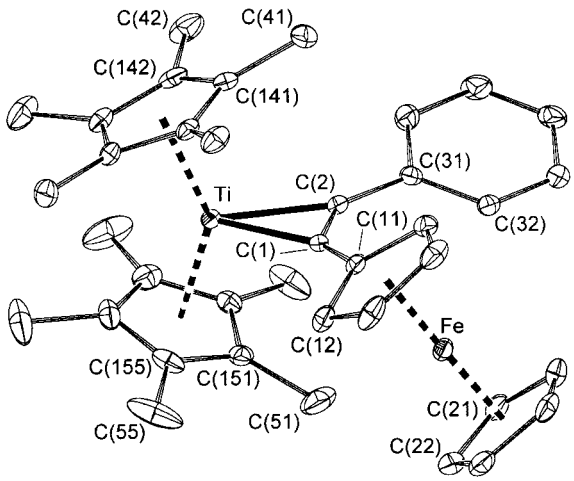

Figure 2. Molecular structure of **9** showing the atom-labeling scheme. Thermal ellipsoids are drawn at the 30% probability level. For clarity, all hydrogen atoms were omitted.

Table 2. Selected Bond Lengths [Å], Bond Angles [deg], and Dihedral Angles[a] [deg] for 9

Ti−C(1)	2.088(3)	C(1)−Ti−C(2)	36.5(1)
Ti−C(2)	2.093(3)	Ti−C(2)−C(31)	150.5(3)
C(1)−C(2)	1.312(5)	Ti−C(1)−C(11)	146.2(2)
C(1)−C(11)	1.455(5)	C(1)−C(2)−C(31)	138.0(3)
C(11)−C(12)	1.419(5)	C(2)−C(1)−C(11)	139.4(3)
C(2)−C(31)	1.461(5)		
C−C(Ph) av	1.389(9)	C−C−C(Ph) av	120(2)
C(11)−C(1)−C(2)−Si	15.8(7)		

	$(C_5Me_5)_2Ti$	Cp_2Fe
CE−CE	3.973(2)	3.312(2)
M−CE	2.110(2), 2.106(2)	1.657(2), 1.657(2)
M−C(Cp)	2.398(3)−2.453(3)	2.034(4)−2.091(3)
M−C(Cp) av	2.43(2)	2.05(2)
C−C(Cp) av	1.412(9)	1.42(1)
$C_{Cp}-C_{Me}$ av	1.500(8)	
∠(Cp,Cp)	40.1(2)	5.3(3)
CE−M−CE	140.8(5)	176.3(7)
C−C−C(Cp) av	108.0(4)	108.0(8)

[a] CE denotes the centroid of the corresponding cyclopentadienyl ring.

Scheme 3. Catalytic Dimerization of TMSA

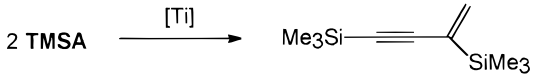

10

Catalytic Dimerization of TMSA. Since the permethyltitanocene−bis(trimethylsilyl)acetylene complex has been found an excellent catalyst for selective head-to-tail dimerization of various terminal acetylenes,[13,14] its analogues **6** and **9** were also tested for catalytic activity toward dimerization of TMSA (Scheme 3). When reacted with an excess of TMSA at 60 °C, compound **9** afforded selectively head-to-tail dimer $(TMSA)_2$, 2,4-bis(trimethylsilyl)but-1-ene-3-yne (**10**), in quantitative yield with no admixture of isomeric dimers, cyclotrimers, and linear oligomers of TMSA, while complex **6** showed no catalytic activity. However, the turnover number of 62.5 mol TMSA/mol **9** is considerably lower than that of (η^5-

(11) Allen, F. H.; Kennard, O.; Watson, D. G.; Brammer, L.; Orpen, A. G.; Taylor, R. *J. Chem. Soc., Perkin Trans. 2* **1987**, S1.
(12) Gyepes, R.; Štěpnička, P. Structure submitted to the Cambridge Crystallographic Data Centre (reference number 961209L).
(13) Varga, V.; Petrusová, L.; Čejka, J.; Hanuš, V.; Mach, K. *J. Organomet. Chem.* **1996**, *509*, 235.
(14) Varga, V.; Petrusová, L.; Čejka, J.; Mach, K. *J. Organomet. Chem.* **1997**, *532*, 251.

$C_5Me_5)_2Ti(\eta^2\text{-}Me_3SiC{\equiv}CSiMe_3)$, in which case turnover numbers up to 1500 were observed.[13] Since all mentioned complexes bear the permethylated titanocene moiety, the presence of which is essential for the selective head-to-tail dimerization of terminal acetylenes, the differences in their reactivity come most likely from different stereoelectronic properties of the coordinated acetylenes. The inertness of **6** toward TMSA (proved by UV/vis spectra) allows us to conclude that different activities of **6** and **9** result plausibly from different abilities of the parent complexes to release the coordinated alkyne under TMSA attack, affording the active species.

Concluding Remarks

The novel titanocene−ferrocene bimetalic complexes **4**−**6**, **8**, and **9**, possessing the metalocene units joined through the carbon atoms of the η^2-coordinated triple bond, are accessible in high yields by the magnesium-reduction method. The yield of complex **7** is poor due to a competitive reduction of acetylene **3**, affording (*E*)-FcCH=CHPh and $FcCH_2CH_2Ph$. The crystal structures of **5** and **9** and NMR and IR spectra of all the complexes indicate a titanacyclopropene-like coordination of the acetylenes to the titanocene frame with various degrees of deviation from the regular arrangement due to the steric requirements of both the alkyne and the titanocene units. Complexes **6** and **9** were tested as the catalysts for dimerization of TMSA. The fact that complex **9** is an efficient catalyst for selective head-to-tail dimerization of TMSA whereas its analogue **6** is inactive points to a key role of the alkyne substituents in determination of catalytic activity. However, further investigations at steric and electronic properties of coordinated internal acetylenes which control their replacement by a terminal acetylene in the first step of the catalytic cycle are required.

Experimental Section

General Comments. NMR spectra were recorded at room temperature in C_6D_6 or $CDCl_3$ solutions on Varian Unity 200 (^{1}H, 200.06 MHz), Varian Unity 500 (^{13}C, 125.70 MHz), or Varian Unity Inova 400 instruments (^{1}H, 399.95 MHz; ^{13}C, 100.58 MHz). Chemical shifts (δ, ppm) are given relative to the solvent signal (C_6D_6: δ_H 7.15, δ_C 128.0 ppm) or to internal tetramethylsilane. ^{29}Si NMR spectra were obtained by using the standard DEPT pulse sequence (79.46 MHz) and are referenced to external tetramethylsilane. Mass spectra were measured on VG 7070E and JEOL HX-110 instruments (EI, 70 eV, direct inlet at the temperature given below). IR spectra in Nujol mulls were obtained on an FT IR ATI Mattson Genesis instrument; those in KBr pellets or in hexane solutions were recorded on a Specord 75 IR spectrometer (Carl Zeiss, Jena, Germany). UV/vis spectra were measured on a Varian Carry 17D spectrometer using a pair of all-sealed quartz cells (Hellma; $d = 0.1$ and 1.0 cm). All manipulations with titanocene complexes **4**−**9** were performed using all-sealed glass devices on an all-glass high-vacuum line equipped with breakable seals. Diethyl ether was freshly distilled from potassium. Hexane and THF were refluxed with $LiAlH_4$ and distilled onto dimeric titanocene, $(\mu\text{-}\eta^5\text{:}\eta^5\text{-}C_{10}H_8)[(\eta^5\text{-}C_5H_5)Ti(\mu\text{-}H)]_2$.[15] THF, hexane, and C_6D_6 were stored as solutions of dimeric titanocene on vacuum line. TMSA (Aldrich, 98%) was carefully degassed in a vacuum and mixed with dimeric titanocene. After standing for ca. 2 h, purified TMSA was distilled from a khaki green solution and stored on a vacuum line. If the mixture of TMSA and dimeric titanocene turned red, TMSA was distilled to a batch of fresh dimeric titanocene. This step was repeated until the resulting mixture remained green. Ethynylferrocene, **1**, was synthesized from acetylferrocene. Diethylamine (99+%, Fluka), iodobenzene (Fluka), and magnesium (for Grignard reactions, Fluka) were used as received. In some cases, activated magnesium was applied. It resulted as the rest from preparation of titanocene η^2-bis(trimethylsilyl)acetylene complexes and was washed with THF and dried in a vacuum before use.

[(Trimethylsilyl)ethynyl]ferrocene, 2. In an argon atmosphere, the solution of **1** (2.10 g, 10.0 mmol) in dry diethyl ether (50 mL) was cooled to −20 °C, and *n*-BuLi (7.5 mL 1.6 M in hexanes, 12 mmol) was added slowly. The resulting mixture was stirred at −20 °C for 30 min and cooled to −50 °C, and neat Me_3SiCl (1.6 mL, 13 mmol) was introduced dropwise while stirring. The mixture was allowed to warm to room temperature with continuous stirring for 1 h (after 15 min formation of a white precipitate started). After quenching with saturated aqueous $NaHCO_3$ (20 mL), the organic phase was separated, washed with water (3 × 20 mL), dried over $MgSO_4$, and evaporated. The crude product was chromatographed on an alumina column with petroleum ether (bp 40−60 °C) as the eluent. Evaporation of the first band gave **2** as an orange solid. Yield: 2.75 g (97%). ^{1}H NMR (400 MHz, $CDCl_3$, Me_4Si; cf. ref 17): δ 0.22 (s, 9 H, *Me*$_3$Si), 4.16 (apparent t, 2 H, C_5H_4), 4.17 (s, 5 H, *Cp*), 4.42 (apparent t, 2 H, C_5H_4). ^{13}C (100 MHz, $CDCl_3$, Me_4Si): δ 0.2 (*Me*$_3$Si), 64.8 (C_{ipso}, C_5H_4), 68.7 (CH; C_5H_4), 70.1 (CH; *Cp*), 71.7 (CH; C_5H_4), 90.5, 104.2 (*C*≡*C*). IR (KBr, cm^{-1}): 3098 (w), 3087 (w), 2953 (m), 2139 (vs), 1409 (m), 1258 (s), 1248 (vs), 1104 (s), 1060 (m), 1037 (m), 1019 (s), 1002 (s), 923 (s), 860 (sh), 850 (vs), 840 (sh), 825 (vs), 759 (s), 722 (m), 699 (m), 539 (m), 506 (m), 487 (m), 476 (s), 455 (m). EI MS (65 °C): *m*/*z* (relative abundance) 284 (6), 283 (23), 282 ($M^{\bullet+}$, 100), 280 (6), 267 ($[M - Me]^+$, 20), 133.5 ($[M - Me]^{2+}$, 13), 121 ($[C_5H_5Fe]^+$, 7), 73 (Me_3Si^+, 4), 56 ($Fe^{\bullet+}$, 7). UV/vis (hexane, nm): 330 (sh) ∼ 440. Anal. Calcd for $C_{15}H_{18}FeSi$: C, 63.83; H, 6.43. Found: C, 64.05; H, 6.52.

[Phenyl(ethynyl)]ferrocene, 3. Complex $[Pd(PPh_3)_2Cl_2]$ (72 mg, 0.1 mmol), CuI (21 mg, 0.1 mmol), and iodobenzene (2.10 g, 10 mmol) were suspended in diethylamine (50 mL) and carefully degassed by several vacuum-argon cycles. To the resulting clear solution was added **1** (2.11 g, 10 mmol), and the mixture was stirred at room temperature for 16 h. Excess amine was evaporated under reduced pressure, and the solid residue was chromatographed on a silica column using 20% (*v*/*v*) diethyl ether in hexane as the eluent. Evaporation of the first colored band afforded **3** as a

(15) Antropiusová, H.; Dosedlová, A.; Hanuš, V.; Mach, K. *Transition Met. Chem*. **1981**, *6*, 90.

(16) (a) Rosenblum, M.; Brawn, N.; Papenmeier, J.; Applebaum, M. *J. Organomet. Chem*. **1966**, *6*, 173. (b) Rosenblum, M.; Brawn, N. M.; Ciappenelli, D.; Tancrede, J. *J. Organomet. Chem*. **1970**, *24*, 469.

(17) Pudelski, J. K.; Callstrom, M. R. *Organometallics* **1994**, *13*, 3095.

rusty-brown solid. Yield: 2.55 g (89%). ^{1}H NMR (400 MHz, $CDCl_3$, Me_4Si; cf. ref 18): δ 4.23 (apparent t, 2 H, C_5H_4), 4.24 (s, 5 H, *Cp*), 4.50 (apparent t, 2 H, C_5H_4), 7.27−7.35 (m, 3 H, *Ph*), 7.46−7.51 (m, 2 H, *Ph*). ^{13}C (100 MHz, in $CDCl_3$, Me_4Si): δ 65.2 (C_{ipso}, C_5H_4), 68.8 (CH, C_5H_4), 69.9 (CH, *Cp*), 71.4 (CH, C_5H_4), 85.7, 88.3 (*C*≡*C*); 123.9 (C_{ipso}, *Ph*), 127.6, 128.3, 131.4 (CH, *Ph*). IR (KBr, cm^{-1}): 3090 (w), 3050 (w), 2220 (m), 2204 (m), 1594 (m), 1490 (s), 1437 (s), 1407 (m), 1202 (m), 1100 (s), 1066 (m), 1023 (s), 996 (s), 921 (m), 820(vs), 811 (s), 754 (vs), 694 (s), 543 (s), 514 (m), 498 (vs), 485 (s). EI MS (120 °C): *m*/*z* (relative abundance) 287 (21), 286 ($M^{\bullet+}$, 100), 284 (7), 228 (8), 165 ([M − C_5H_5Fe]$^+$, 16), 164 (5), 152 (5), 143(7), 121 ([C_5H_5Fe]$^+$, 17), 56 ($Fe^{\bullet+}$, 18). UV/vis (hexane, nm): 443. Anal. Calcd for $C_{18}H_{14}Fe$: C, 75.55; H, 4.93. Found: C, 75.14; H, 4.91.

[(η^5-C_5H_5)$_2$Ti(η^2-FcC≡CSiMe$_3$)], 4. Complex (η^5-C_5H_5)$_2$$TiCl_2$ (0.249 g, 1 mmol), magnesium turnings (0.024 g, 1 mmol), and **2** (0.282 g, 1 mmol) were charged into the reaction ampule equipped with breakable seals and evacuated, and THF (20 mL) was added on a vacuum line. The mixture was stirred at room temperature for 3 days to give a red-brown solution, while all the magnesium had dissolved. THF was evaporated in a vacuum at finally 60 °C to leave a brown solid. This was extracted by hexane to remove $MgCl_2$ until the extract remained pale yellow. Cooling of the concentrated extract to −10 °C afforded 0.35 g (77%) of **4** as red-brown crystals. ^{1}H NMR (200 MHz, C_6D_6): δ −0.15 (s, 9 H, *Me*$_3$Si), 3.10, 3.86 (2 × aparent t, 2 H, C_5H_4Fe); 4.17 (s, 5 H, C_5H_5Fe), 6.35 (s, 10 H, C_5H_5Ti). ^{13}C NMR (125 MHz, C_6D_6): δ −0.1 (*Me*$_3$Si), 68.2 (CH, C_5H_4Fe), 69.5 (CH, C_5H_5Fe), 70.0 (CH, C_5H_4Fe), 85.8 (C_{ipso}, C_5H_4Fe), 113.3 (CH, C_5H_5Ti), 208.6, 218.4 (η^2-*C*≡*C*). EI MS (direct inlet, 70 eV, 130 °C): *m*/*z* (relative abundance) 460 ($M^{\bullet+}$, 1), 282 (75), 267 (12), 178 (100), 133.5 (11), 121 (13), 113 (19), 73 (8), 56 (14). IR (hexane, cm^{-1}): 1713 (m, sh), 1685 (m), 1237 (s), 1216 (m), 1102 (m), 1010 (s), 927 (m), 848 (vs), 831 (vs), 810 (vs), 788 (vs), 745 (m), 682 (m), 655 (m), 646 (m), 532 (m), 488 (m), 480 (m), 470 (m), UV/vis (hexane, nm): 450 (sh) ≫ 880 (br).

[(η^5-C_5HMe_4)$_2$Ti(η^2-FcC≡CSiMe$_3$)], 5. Complex (η^5-C_5HMe_4)$_2$$TiCl_2$ (0.361 g, 1.0 mmol) and **2** (0.282 g, 1 mmol) were charged into an ampule and evacuated on a vacuum line. THF (20 mL) and activated Mg (0.2 g, 8.3 mmol) were added, and the mixture was stirred at room temperature. The color of the solution rapidly turned from brown to blue and then, within 10 min, to orange-brown. After standing overnight, the solution was separated from excess magnesium and the THF was evaporated. The brown residue was extracted by hexane to give an orange-brown solution. Slow evaporation of the solvent gave brown crystals of **5**. They were washed with a small amount of hexane and dried in a vacuum. Yield: 0.49 g (87%). ^{1}H NMR (200 MHz, C_6D_6): δ 0.17 (s, 9 H, *Me*$_3$Si), 1.32, 1.49, 2.08, 2.09 (4 × s, 6 H, *Me*$_4$$C_5H$); 3.28, 3.90 (2 × aparent t, 2 H, C_5H_4); 4.16 (s, 5 H, C_5H_5), 5.31 (s, 2 H, Me_4C_5H). ^{13}C NMR (125 MHz, C_6D_6): δ −0.1 (*Me*$_3$Si), 13.1, 13.2, 13.4, 13.8 (*Me*$_4$$C_5H$); 67.3 (CH, C_5H_4Fe), 69.4 (CH, C_5H_5), 70.1 (CH, C_5H_4), 86.3 (C_{ipso}, C_5H_4), 112.4 (CH, Me_4C_5H), 120.1, 120.8, 123.8, 126.4 (C, Me_4C_5H); 210.9, 217.8 (η^2-*C*≡*C*). EI-MS (direct inlet, 70 eV, 160 °C): *m*/*z* (relative abundance) 572 ($M^{\bullet+}$, 0.04), 290 (87), 282 (100), 267 (16), 133.5 (15), 121 (12), 73 (8), 56 (13). IR (hexane, cm^{-1}): 1644 (m), 1625 (m, sh), 1237 (s), 1103 (m), 1018 (m), 997 (m), 924 (m), 846 (vs), 825 (vs), 811 (vs), 746 (m), 662 (m), 540 (s), 492 (m), 480 (m), 468 (m), 420 (m). UV/vis (hexane, nm): 475 (sh) ≫ 805 (br). Anal. Calcd for $C_{33}H_{44}FeSiTi$: C, 69.23; H, 7.75. Found: C, 69.54; H, 7.79.

[(η^5-C_5Me_5)$_2$Ti(η^2-FcC≡CSiMe$_3$)], 6. The procedure described for synthesis of **5** was followed starting from (η^5-C_5Me_5)$_2$$TiCl_2$ (0.389 g, 1 mmol), **2** (0.282 g, 1 mol), and activated Mg (0.2 g, 8.3 mmol). Isolation as described above afforded orange-brown crystalline complex **6**. Yield: 0.51 g (84%). ^{1}H NMR (200 MHz, C_6D_6): δ 0.22 (s, 9 H, *Me*$_3$Si), 1.81 (s, 30 H, *Me*$_5$$C_5$), 3.98 (s, 5 H, C_5H_5Fe), 4.02, 4.28 (2 × apparent t, 2 H, C_5H_4Fe). ^{13}C NMR (125 MHz, C_6D_6): δ 0.3 (*Me*$_3$Si), 11.4 (*Me*$_5$$C_5$), 69.2, 69.3 (2 × CH, C_5H_4Fe); 69.4 (CH, C_5H_5Fe), 85.0 (C_{ipso}, C_5H_4Fe), 121.1 (Me_5C_5), 212.6, 218.3 (η^2-*C*≡*C*). EI MS (direct inlet, 70 eV, 200 °C): *m*/*z* (relative abundance) 600 ($M^{\bullet+}$, 0.01), 318 (73), 282 (100), 267 (16), 133.5 (13), 121 (6), 56 (6). IR (hexane, cm^{-1}): 3093 (m, b), 1627 (s, b), 1258 (s), 1241 (s), 1208 (m), 1107 (s), 1073 (s), 1022 (s), 1001 (m), 928 (m), 851 (vs), 831 (vs), 816 (vs), 545 (s), 495 (m), 472 (m), 431 (s). UV/vis (hexane, nm): 480 ≫ 810 (br).

[(η^5-C_5H_5)$_2$Ti(η^2-FcC≡CPh)], 7. Complex (η^5-C_5H_5)$_2$-$TiCl_2$ (0.249 g, 1.0 mmol), **3** (0.286 g, 1.0 mmol), magnesium (0.024 g, 1.0 mmol), and THF (20 mL) were heated in a sealed ampule to 60 °C for 10 h. THF was removed in a vacuum, and the resulting brown residue was extracted with hexane. Evaporation of the hexane extract gave only a mixture of (*E*)-FcCH═CHPh and $FcCH_2CH_2Ph$ containing **7** as the minor component. All attempts to obtain pure **7** were unsuccessful. ^{1}H NMR (400 MHz, C_6D_6): δ 2.83, 3.80 (2 × apparent t, 2 H, C_5H_4); 4.04 (s, 5 H, C_5H_5Fe), 6.42 (s, 5 H, C_5H_5Ti), 6.96−7.20 (m, 5 H, *Ph*). EI MS (direct inlet, 70 eV, 120 °C): *m*/*z* 464 ($M^{\bullet+}$), 178 ([$C_{10}H_{10}Ti$]$^+$), 286 (**3**$^{\bullet+}$) observed after evaporation of volatile FcCH═CHPh and $FcCH_2CH_2Ph$ from the sample directly in the probe.

[(η^5-C_5HMe_4)$_2$Ti(η^2-FcC≡CPh)], 8. Complex (η^5-C_5HMe_4)$_2$$TiCl_2$ (0.361 g, 1.0 mmol), **3** (0.286 g, 1 mmol), and activated Mg (0.2 g, 8.3 mmol) were reacted in THF (20 mL) at 60 °C for 30 min. THF was evaporated in a vacuum, and the orange-brown residue was extracted by hexane. Evaporation of hexane afforded a yellow-brown waxy solid. Yield: 0.53 g (92%). ^{1}H NMR (400 MHz, C_6D_6): δ 1.46, 1.47, 2.02, 2.07 (4 × s, 6 H, *Me*$_4$$C_5H$); 3.67, 4.00 (2 × br apparent t, 2 H, C_5H_4); 4.23 (s, 5 H, C_5H_5), 5.16 (s, 2 H, Me_4C_5H), 6.97−7.24 (m, 5 H, *Ph*). ^{13}C NMR (100 MHz, C_6D_6): δ 13.3, 13.3, 13.5, 13.7 (*Me*$_4$$C_5H$); 67.3, 68.9 (CH, C_5H_4); 69.2 (C_5H_5), 86.6 (C_{ipso}, C_5H_4), 111.9 (CH, Me_4C_5H), 120.5, 120.9 (C, Me_4C_5H); 125.1 (CH, *Ph*), 126.0, 126.0 (C, Me_4C_5H); 130.6 (CH, *Ph*), 140.1 (C_{ipso}, *Ph*), 195.7, 199.1 (η^2-*C*≡*C*); one of the *C*H carbons of the phenyl group is overlapped by the solvent signal. EI MS (140 °C): *m*/*z* (relative abundance) 576 ($M^{\bullet+}$, 0.7), 290 (100), 286 (9). IR (hexane, cm^{-1}): 3087 (m), 1757 (w), 1661 (m, b), 1589 (s), 1329 (w), 1309 (w), 1252 (m), 1107 (s), 1071 (m), 1025 (s), 1000 (s), 974 (w), 930 (w), 913 (w), 896 (m), 860 (w),

(18) Rausch, M. D.; Siegel, A.; Klemann, L. P. *J. Org. Chem.* **1966**, *31*, 2703.

827 (sh), 815 (vs), 759 (m), 700 (vs), 493 (s), 422 (m). UV/vis (hexane, nm): 470(sh) ≫ 710.

[(η^5-C_5Me_5)$_2$Ti(η^2-FcC≡CPh)], 9. Following the procedure for preparation of **8**, (η^5-C_5Me_5)$_2$TiCl$_2$ (0.389 g, 1 mmol), **3** (0.286 g, 1 mmol), and activated magnesium (0.2 g, 8.3 mmol) gave crude **9** as a brown residue after evaporation of THF. The residue was extracted by 50 mL of hexane to afford a brown-yellow solution, which deposited brown crystals of pure **9** after cooling to −18 °C. Yield: 0.51 g (85%), mp 101 °C. ^{1}H NMR (400 MHz, C_6D_6): δ 1.25 (s, 30 H, *Me*$_5$C$_5$), 3.21, 3.52 (2 × apparent t, 2 H, C$_5$*H*$_4$); 3.76 (s, 5 H, C$_5$*H*$_5$), 6.62−6.75 (m, 5 H, *Ph*). ^{13}C (100 MHz, C_6D_6): δ 12.4 (*Me*$_5$C$_5$), 67.1, 68.9 (CH, C$_5$H$_4$); 69.3 (*C*$_5$H$_5$), 87.4 (C$_{ipso}$, C$_5$H$_4$), 121.8 (Me$_5$*C*$_5$), 124.9, 127.9, 130.8 (CH, *Ph*); 140.4 (C$_{ipso}$, *Ph*), 195.1, 198.5 (η^2-*C*≡*C*). EI MS (180 °C): *m*/*z* (relative abundance) 604 ($M^{\bullet+}$, 0.07), 318 (100), 286 (15). IR (KBr, cm^{-1}): 3092 (w), 2970 (m), 2897 (s), 2848 (m), 1651 (m), 1585 (s), 1435 (s, b), 1375 (vs), 1106 (s), 1025 (s), 1001 (s), 812 (vs), 760 (s), 698 (vs), 600 (m), 587 (m), 500 (m), 488 (s), 480 (s), 464 (m). UV/vis (hexane, nm): 520 (sh) ≫ 725. Anal. Calcd for $C_{38}H_{44}FeTi$: C, 75.50; H, 7.34. Found: C, 75.43; H, 7.29.

Reactivity of 6 and 9 toward TMSA. Compounds **6** and **9**, respectively (0.1 g, 0.16 mmol), were dissolved in hexane (2 mL), TMSA (1.5 mL, 10 mmol) was added, and the mixture was kept at 60 °C in a vessel equipped with an all-sealed quartz cell (Hellma, 0.2 cm). The course of the reaction was monitored by UV/vis−NIR spectroscopy every ca. 4 h in order to check the concentrations of **6** (λ 810 nm) and **9** (λ 725 nm), respectively, and the concentration of unreacted TMSA (λ 1540 nm; 2 × ν(C−H)). Upon additon of TMSA to complex **6**, the concentration of the titanocene complex decreased by ca. 10%, and the content of TMSA remained unchanged even after heating to 60 °C for 100 h. For **9**, the band of the starting titanocene complex disappeared completely after 8 h at 60 °C, the acetylene being completely consumed within 20 h. The volatiles from reaction of **9** with excess TMSA were separated by vacuum distillation at ambient temperature and collected in a trap cooled by liquid nitrogen (overnight). GC−MS and NMR analysis of the distillation product revealed the presence of 2,4-bis(trimethylsilyl)but-1-en-3-yne, Me$_3$SiC≡CC(SiMe$_3$)=CH$_2$ (**10**), as the sole product. ^{1}H NMR (400 MHz, C_6D_6): δ 0.13, 0.18 (2 × s, 9 H, *Me*$_3$Si); 5.54, 6.13 (2 × d, 1 H, $^2J_{HH}$ = 3.4 Hz, =C*H*$_2$). ^{13}C NMR (100 MHz, C_6D_6): δ −2.2, 0.2 (*Me*$_3$Si); 98.7, 107.2 (*C*≡*C*); 134.9 (=*C*H$_2$), 135.3 (=*C*(SiMe$_3$)−). ^{29}Si DEPT (C_6D_6): −18.5 (s, C≡C*Si*Me$_3$), −2.2 (s, C=C*Si*Me$_3$).

Crystal Structure Determination. X-ray-quality crystals of **5** and **9** were grown by a slow evaporation of their hexane solutions. For both complexes, the selected specimen was inserted into a Lindenmann-glass capillary and sealed by wax in a glovebox. The diffractions were measured on a four-circle diffractometer, CAD4-MACHIII, at 296(1) and 150.0(1) K for **5** and **9**, respectively, using graphite-monochromated Mo Kα radiation (λ = 0.710 73 Å) and θ−2θ scan. Three standard diffractions monitored every 1 h showed no significant intensity variation (≤4%). The lattice parameters were refined by least-squares fitting from 25 automatically centered diffractions with 15° ≤ θ ≤ 16° (**5**) and 13° ≤ θ ≤ 13.5° (**9**).

Table 3. Crystallographic Data, Data Collection, and Structure Refinement for 5 and 9[a]

	5	**9**
formula	$C_{33}H_{44}FeSiTi$	$C_{38}H_{44}FeTi$
M	572.52	604.48
T (K)	296(1)	150.0(1)
cryst syst, space group	monoclinic, $P2_1/n$ (No. 14)	monoclinic, $P2_1/c$ (No. 14)
a (Å)	15.342(3)	16.617(3)
b (Å); β (deg)	11.162(3); 105.57(2)	12.494(2); 98.51(1)
c (Å)	18.501(3)	14.892(2)
V (Å^3); *Z*	3052(1); 4	3057.7(8); 4
D_{calc} (g mL^{-1})	1.246	1.313
μ (mm^{-1})	0.795	0.761
color, habit	orange-brown, bar	red-brown, prism
cryst dimens (mm^3)	0.39 × 0.50 × 0.61	0.29 × 0.43 × 0.50
no. of diffractions collected; 2θ range (deg)	7005; 2θ ≤ 50.0	4982; 2θ ≤ 48.0
h, *k*, *l* range	±*h* +*k* ±*l*	±*h* ±*k* ±*l*
no. of unique diffractions	5368	4784
no. of observed diffractions; $\|F_o\| > 4\sigma(F_o)$	4045	4368
F(000)	1216	1280
no. of refined params	501	418
$(\Delta/\sigma)_{max}$	0.00	0.00
R(*F*), *wR*(F^2) (%); *S* for all diffractions	5.99, 9.19; 1.03	5.18, 12.90; 1.05
R(*F*), *wR*(F^2) (%) for observed diffractions	3.33, 8.13	4.26, 11.71
R(σ) (%)	3.32	1.88
$\Delta\rho$ (e Å^{-3})	0.23; −0.25	0.37; −0.47

[a] $R(F) = \sum||F_o| - |F_c||/\sum|F_o|$, $wR(F^2) = [\sum(w(F_o^2 - F_c^2)^2)/(\sum w(F_o^2)^2)]^{1/2}$, $S = [\sum(w(F_o^2 - F_c^2)^2)/(N_{diffrs} - N_{params})]^{1/2}$, $R(\sigma) = \sum\sigma(F_o^2)/\sum F_o^2$.

The structure of **5** was solved by direct methods (SIR92, ref 19), yielding the positions of all non-hydrogen atoms. Hydrogen atoms were identified on the difference electron density map and freely isotropically refined. The full-matrix least-squares refinement was carried out by minimization of the function $\sum w(|F_o| - |F_c|)^2$ (SHELXL93, ref 20), where $w = [\sigma^2(F_o^2) + (0.0487P)^2 + 0.9775P]^{-1}$ and $P = (F_o^2 + 2F_c^2)/3$.

The crystal of **9** used for the collection of diffraction data suffered from nonmerohedral twinning, therefore the correction according to the method of Pratt[21] et al. and Jameson[22] et al. was included in the refinement. From the twin law,

$$\begin{pmatrix} h^{II} \\ k^{II} \\ l^{II} \end{pmatrix} = \begin{pmatrix} -1 & 0 & 1/3 \\ 0 & -1 & 0 \\ 0 & 0 & -1 \end{pmatrix} \begin{pmatrix} h^{I} \\ k^{I} \\ l^{I} \end{pmatrix}$$

it follows that the two domains contribute to the diffractions with $l = 3n$. The refined fractions of these domains were 0.635 and 0.365. The structure was solved by direct methods (SIR92) followed by least-squares refinement on F^2 (SHELXL97, ref 23); the weighting scheme applied was $\sum w(|F_o| - |F_c|)^2$, where $w = [\sigma^2(F_o^2) + (0.0730P)^2 + 4.2468P]^{-1}$ and $P = (F_o^2 + 2F_c^2)/3$. All

(19) Altomare, A.; Burla, M. C.; Camalli, M.; Cascarano, G.; Giacovazzo, C.; Guagliardi, A.; Polidori, G. *J. Appl. Crystallogr.* **1994**, *27*, 435.
(20) Sheldrick, G. M. *SHELXL93. Program for Crystal Structure Refinement from Diffraction Data;* University of Göttingen: Göttingen, Germany, 1993.
(21) Pratt, C.; Coyle, B. A.; Ibers, J. A. *J. Chem. Soc.* **1971**, 2146.
(22) Jameson, G. B.; Schneider, R.; Dubler, E.; Oswald, H. R. *Acta Crystallogr., Sect. B* **1982**, *B38*, 3016.
(23) Sheldrick, G. M. *SHELXL97. Program for Crystal Structure Refinement from Diffraction Data;* University of Göttingen: Göttingen, Germany, 1997.

the non-hydrogen atoms were refined anisotropically. Aromatic hydrogens (phenyl, ferrocenyl) were found on difference electron density maps and isotropically refined. Methyl hydrogen atoms were included in theoretical positions and assigned C−H 0.96 Å and $U_{iso}(H) = 1.2U_{eq}(C)$. Further details on data collection and refinement as well as relevant crystallographic data are given in Table 3.

Acknowledgment. Support for this research was provided by the Grant Agency of the Czech Republic (Grant Nos. 203/96/0948 and 203/97/0242). The Grant Agency of the Czech Republic (Grant No. 203/96/0111) also sponsored access to the Cambridge Crystallographic Data Centre.

Supporting Information Available: Tables of crystallographic data, atomic coordinates, thermal parameters, intramolecular distances and angles, dihedral angles of least-squares planes, and packing diagrams for **5** and **9**. This material is available free of charge via the Internet at http://pubs.acs.org.

OM980832U